



Brief communication: Real-time estimation of optimal tip-speed ratio for controlling wind turbines with degraded blades

Devesh Kumar^{1,2} and Mario A. Rotea³

¹Center for Wind Energy and Department of Electrical and Computer Engineering, The University of Texas at Dallas, Richardson, TX 75080 USA.

²Now with Drive System Design Inc., Farmington Hills, MI 48335, USA

³Center for Wind Energy and Department of Mechanical Engineering, The University of Texas at Dallas, Richardson, TX 75080 USA.

Correspondence: Mario A. Rotea (rotea@utdallas.edu)

Abstract. Rotor performance is adversely affected by wear and tear of blade surfaces caused, for example, by rain, snow, icing, dirt, bugs, ageing, etc. Blade surface degradation changes the aerodynamic properties of the rotor, which in turn changes the optimal tip-speed ratio (TSR) and the corresponding maximum power coefficient. Below rated wind speed, if a turbine continues to operate at the manufacturer designed optimal TSR, the rotor power could decrease more than necessary unless the optimal TSR is corrected to compensate for blade degradation or other off-design conditions. Re-tuning the tip-speed ratio in these off-design conditions can lead to an improvement in energy capture. In this work, we describe a real-time algorithm to re-tune the tip-speed ratio to its optimal, but unknown, value under blade degradation. The algorithm uses power measurements only and a Log-of-Power Proportional-Integral Extremum Seeking Control (LP-PIESC) strategy to re-tune the TSR. The value of this algorithm is demonstrated using it to command the TSR set-point required by a generator speed control loop that maximizes power generated below rated wind speeds. Comparison of this solution with a baseline controller that uses the optimal TSR for a rotor with clean blades demonstrates improvements in energy capture between 0.5% and 3.4%, depending on the severity of blade degradation and the wind conditions. These results are obtained using the OpenFAST simulation tool, the NREL 5-MW reference turbine and the Reference Open-Source Controller developed by the US National Renewable Energy Laboratory.

1 Introduction

Wind turbines produce power in two different regimes: (i) above-rated wind speed, where the machine is controlled to track rated power, and (ii) below-rated wind speed, where the rotor speed is actively controlled to maximize the power extracted from the wind. In the below-rated regime, the rotor power is proportional to the power available in the wind times the power coefficient (C_P). The parameter C_P can be optimized to maximize the output power. For a typical variable-speed variable-pitch wind turbine, C_P is a unimodal function of the tip-speed ratio (λ) and the



blade-pitch angle (β) (Manwell et al., 2010; Burton et al., 2011). This implies that there is an optimal tip-speed ratio and blade-pitch angle for maximizing C_P and hence the output power. Intuitively, maximizing power below-rated wind speeds requires keeping the blade-pitch angle constant at its ideal value β_{opt} while adjusting the rotor speed to
25 maintain the optimal tip-speed ratio λ_{opt} despite wind speed changes (Pao and Johnson, 2011; Burton et al., 2011; Abbas et al., 2022).

Rotor performance is adversely affected by wear and tear of blade surfaces caused, for example, by rain, snow, icing, dirt, bugs, ageing, etc. Blade surface degradation changes the aerodynamic properties of the rotor, which in turn changes the optimal tip-speed ratio λ_{opt} and the corresponding maximum power coefficient C_P^{max} . If a turbine
30 continues to operate at the originally designed λ_{opt} , the rotor power can decrease more than necessary unless the optimal tip speed ratio is corrected to compensate for blade degradation. Re-tuning the optimal tip speed ratio in these off-design conditions can lead to an improvement in energy capture.

A brief description of the losses incurred due to blade degradation is in order. Han et al. (2018) showed that contamination and erosion at leading edge of blade tips adversely affect the annual energy production (AEP) of wind
35 turbines. They reported that contamination and erosion can reduce AEP by 2%-3.7%. Ehrmann et al. (2013, 2017); Wilcox et al. (2017) studied the effect of surface roughness on wind turbine performance. Ehrmann et al. (2013) observed that paint roughness leads to a consistent increase in drag compared to a clean configuration. Ehrmann et al. (2017) showed that the maximum lift-to-drag ratio decreases 40% for $140\mu\text{m}$ roughness, corresponding to a 2.3% loss in AEP. AEP losses of 4.9% and 6.8% for a NACA 63₃ – 418 turbine and an NREL S814 turbine, respectively,
40 operating with $200\mu\text{m}$ roughness were observed in Wilcox et al. (2017). Wilcox and White (2016) studied the power loss due to insect contamination on the blades. They did a computer simulation to predict the expected levels and location of insect contamination on the blade surface and developed a tool to simulate insect impingement for various turbine operating conditions. A numerical approach capable of simulating the ice accretion transient phenomenon and its effects on wind turbine performance was presented in Zanon et al. (2018). This reference shows that keeping
45 the tip-speed ratio at its designed optimal value can reduce performance by 3% after the icing event. This brief discussion suggests that re-tuning the turbine’s control parameters to their “new optimal settings” under off-design conditions has the potential to reduce power and AEP losses.

In this work, we explore the use of a recently develop variant of Extremum Seeking Control (ESC) for re-tuning control parameters to maximize power capture for rotors with degraded aerodynamic performance. More specifically,
50 we apply the Log-of-Power Proportional-Integral Extremum Seeking Control (LP-PIESC) algorithm to identify the optimal tip-speed ratio (TSR) for contaminated or eroded blades in real time. This algorithm requires one measurement only; i.e., the rotor power. The LP-PIESC has been shown to be a faster variant of the traditional perturbation-based ESC (Kumar and Rotea, 2022).

To demonstrate the value of using the LP-PIESC algorithm in these off-design conditions, we apply the TSRs
55 identified with this algorithm as the set-point to be tracked by a generator speed control loop operating below-rated wind speeds. Due to its widespread availability, we have chosen the Reference Open-Source Controller (ROSCO)



developed by Abbas et al. (2022) and the NREL 5-MW reference turbine model (Jonkman et al., 2009) to illustrate our approach.

The main contribution of this work is a practical real-time algorithm (LP-PIESC) to tune the tip-speed ratio set-point of degraded wind turbines utilizing the ROSCO or similar controller.

The organization of the paper is as follows. The ROSCO and the LP-PIESC algorithms are reviewed in Section 2. This section also describes the specific blade degradation cases utilized (blade contamination and erosion). Section 3 focuses on the real-time identification of optimal tip-speed ratio with LP-PIESC, including the algorithm equations. The algorithm parameters are provided in a separate appendix to enhance the manuscript's readability. The results of simulations using OpenFAST (NREL, 2020, accessed: October 10, 2023) for several wind profiles are given in Section 3. These results provide evidence that the LP-PIESC quickly finds the unknown optimal tip-speed ratio despite variations in mean wind speed, turbulence intensity, and the level of blade degradation, thus increasing energy capture in off-design conditions. Conclusions are given in Section 4.

2 Background

2.1 Reference Open-Source Controller (ROSCO)

The Reference Open-Source Controller (ROSCO) has been introduced in Abbas et al. (2022) to update the legacy NREL 5-MW controller (Jonkman et al., 2009). The ROSCO is available for download and implementation on GitHub: <https://github.com/NREL/ROSCO> (accessed on October 10, 2023). This controller is proposed as a modern control architecture that can be deployed on multiple wind turbine models and simplifies the tuning procedure in OpenFAST (NREL, 2020, accessed: October 10, 2023). A high-level block diagram of the ROSCO is shown in Figure 1. In this architecture, both the generator torque (τ_g) and the blade pitch angle (β) are governed by PI controllers. The controller requires a rotor average (effective) wind speed estimator. The optimal tip-speed ratio (λ_{opt}) can be a tunable parameter. Using the optimal tip-speed ratio and estimated wind speed (\hat{v}), a generator speed reference ($\omega_{g,ref}$) is obtained (as per Eq. (1)).

$$\omega_{g,ref} = \frac{\lambda_{opt} \hat{v} N}{R} \quad (1)$$

where R is the rotor radius, and N is the gear ratio. This generator speed reference ($\omega_{g,ref}$) is fed as input to the generator torque PI controller for generator speed (ω_g) control to maximize the power capture in below-rated wind speed. Details of the ROSCO framework can be found in Abbas et al. (2022). In this work, we tune the optimal tip-speed ratio (λ_{opt}) set-point using the LP-PIESC to maximize the power capture below rated wind speed. We did not modify the control logic of the ROSCO and used it as it is defined for the NREL 5-MW reference turbine in OpenFAST. In our simulations, ROSCO takes wind speed estimate \hat{v} from the rotor disk average (RtVAvgxh) calculated by OpenFAST and not from the wind speed estimator inside ROSCO. The reason for this is that the wind speed estimator makes use of the entire power curve, which changes as the blades degrade.

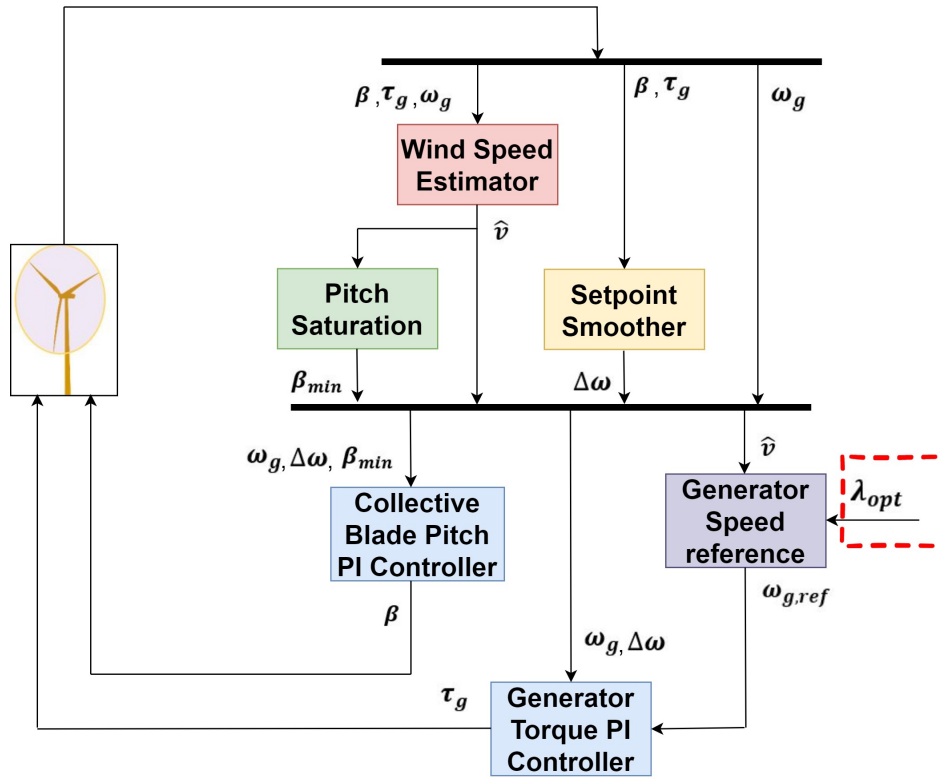


Figure 1. High-level block diagram of Reference Open-Source Controller (ROSCO).

2.2 Performance loss due to leading-edge blade degradation

90 Rotor performance is adversely affected by wear and tear of blade surfaces caused, for example, by rain, snow, icing, dirt, bugs, ageing, etc. Blade surface degradation changes the aerodynamic properties of the rotor, which in turns changes the optimal tip-speed ratio (λ_{opt}) and the corresponding maximum power coefficient (C_p^{max}). If a turbine continues to operate at the designed λ_{opt} , the rotor power can decrease more than necessary unless the optimal tip speed ratio (TSR) is corrected to compensate for blade degradation. Re-tuning the tip-speed ratio in these off-design
 95 conditions can lead to an improvement in energy capture. In this article we demonstrate that extremum seeking control is an effective method to re-tune the optimal TSR.

Han et al. (2018) studied the impact on annual energy production of blade leading edge contamination and erosion. In particular, they studied the aerodynamic performance of the blade tip airfoil (NACA64) for the NREL 5-MW wind turbine (Jonkman et al., 2009). To demonstrate the ability of LP-PIESC for finding the optimal TSR for rotors
 100 with degraded blades, we selected two cases from Han et al. (2018): (i) Contamination of blades - decreased the lift coefficient (C_l) by 30% and increased the drag coefficient (C_d) by 150% and (ii) Erosion of blades - decreased



the lift coefficient (C_l) by 50% and increased the drag coefficient (C_d) by 300%. These changes in lift and drag coefficients occur at angles of attack (AoA) between -5° to 16° . Note that the NACA64 airfoil is in the tip region of the NREL 5-MW turbine blade, approximately 30% of the blade length. A schematic with the degraded blade sector is in Figure 2. Lift and drag coefficients for the clean blade as well as the contaminated and eroded blades are shown in Figure 3.

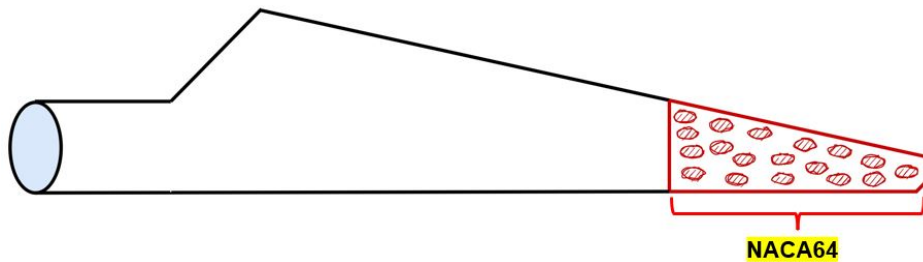


Figure 2. Tip section of the NREL 5-MW blade with NACA64 airfoil. It is 30% of the blade length, 43.05 m from the blade root to 61.5 m.

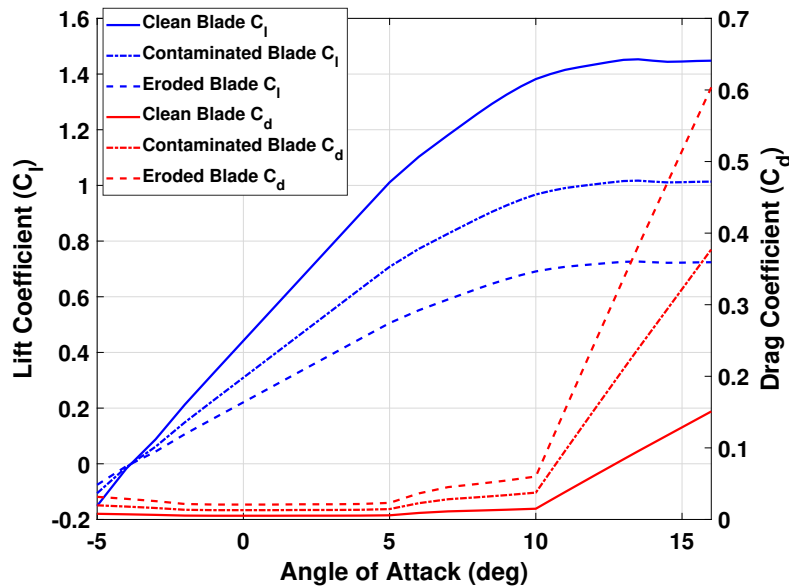


Figure 3. Change of lift and drag coefficients for NACA64 airfoil.

The $C_p - \lambda$ curves with degraded blades were obtained from NREL OpenFAST (NREL, 2020, accessed: October 10, 2023) using the modified lift and drag coefficients. Figure 4 shows the results for all the cases. Note that the optimal values for a clean blade are $\lambda_{opt} = 7.6$ and $C_p^{max} = 0.483$. The modification of the lift and drag coefficients



110 leads to a shift in the optimal $C_P - \lambda$ curve. When the blade is contaminated the optimal TSR increases to $\lambda_{\text{opt}} = 8.2$,
 with $C_P^{\text{max}} = 0.431$. For the eroded blade, the curve shift is more pronounced and the maximum power coefficient
 drops to $C_P^{\text{max}} = 0.351$ at $\lambda_{\text{opt}} = 8.4$. We can observe from these plots that if the turbine is still controlled using the
 clean blade $\lambda_{\text{opt}} = 7.6$ for both the contaminated and degraded blade, it will produce less power than the maximum
 power it could produce should the set-point TSR were changed to their new optimal values. *The C_P loss would*
 115 *be roughly 1.4% for the contaminated blade and 3.5% for the eroded blade if the TSRs are not re-tuned.* Thus, it
 is advantageous to change the set-point TSR to their new optimal values. In this study, the LP-PIESC is used to
 search for these optimal tip-speed ratios.

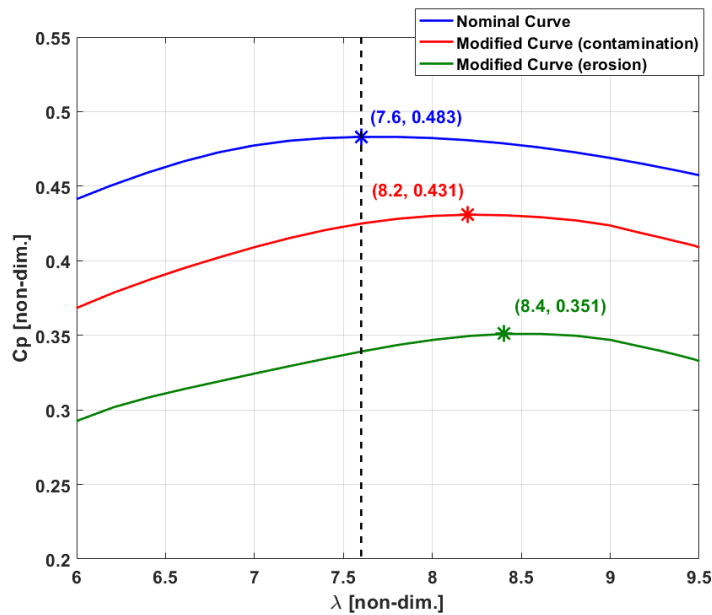


Figure 4. Nominal and modified (due to contamination and erosion of blades) $C_P - \lambda$ curve for NREL 5-MW wind turbine reference model. If the wind turbine continues to operate at the nominally optimal TSR ($\lambda_{\text{opt}} = 7.6$), it would lose more power than necessary as the optimal TSR shifts for degraded blades. Specifically, the C_P loss with respect to the new lower optima would be 1.4% and 3.5% for the contaminated and eroded blade cases, respectively.

2.3 Log-of-Power Proportional-Integral Extremum Seeking Control (LP-PIESC)

120 In this study, we use the Log-of-Power Proportional-Integral Extremum Seeking Control (LP-PIESC) strategy introduced in Kumar and Rotea (2022). The algorithm is gradient-based, which can adjust the tunable parameters to maximize a system's performance index in real-time without any physical models. By perturbing the adjustable parameters with a zero-mean periodic dither signal, the gradient of the performance index with respect to the parameters is estimated. The use of the Log-of-Power (LP) as feedback signal enables consistent convergence across varying

mean wind speeds (Rotea, 2017; Ciri et al., 2019) and PIEESC achieves rapid convergence to the optimum (Guay and Dochain, 2017).

To describe the algorithm used in this study, let us assume that we seek the value of the scalar parameter u that maximizes a scalar-valued function $f(u)$. To solve this problem, the proportional-integral extremum seeking controller proposed in Guay and Dochain (2017) has been modified to add a back-calculation anti-windup and is given by (2):

$$130 \quad \begin{cases} u = -k_p \hat{\theta}_1 + \hat{u} + d(t) \\ \dot{\hat{u}} = -\frac{1}{\tau_I} \hat{\theta}_1 + k_b(u^s - u) \end{cases} \quad (2)$$

where k_p is the proportional gain, τ_I is the integral time constant and k_b is the anti-windup gain. The parameter $\hat{\theta}_1$ is proportional to the gradient $\partial f/\partial u$. The ideal goal is to drive this parameter to zero as quickly as possible. The block diagram for the LP-PIESC with the gradient estimation equations is shown in Figure 5. Note the saturation block to limit the control parameter to safe values and the approximation of any actuator dynamics through the transfer function $F_{in}(s)$. The difference between the saturated output u^s and the calculated controller output u is fed back into the input of the integrator through an anti-windup gain k_b , which is similar to the design of anti-windup ESC proposed in Creaby et al. (2009).

A periodic dither signal $d(t) = a \sin(\omega t)$ is applied to estimate the gradient $\partial f/\partial u$, where a is the dither amplitude, ω is the dither frequency. The parameter to be estimated is $\theta = [\theta_0, \theta_1]^T$ (Guay and Dochain, 2017), where the superscript T denotes transpose. In this study, θ is a real-valued vector of dimension two. We only require the scalar component θ_1 that contains the gradient information; θ_0 is a bias term needed for the parameter estimation to work properly.

A detailed discussion on the LP-PIESC algorithm can be found in Kumar and Rotea (2022).

3 Real-time identification of optimal TSR with LP-PIESC

3.1 LP-PIESC design

3.1.1 System architecture

The NREL 5-MW turbine reference model with OpenFAST is used in the work (Jonkman, 2013). Table 1 lists the major parameters of this turbine model.

The focus of this study is below-rated wind speed, as this is the region where wind turbine control algorithms can maximize power. A high-level block diagram of the entire system is shown in Figure 6. The input to the LP-PIESC is the logarithm of the rotor power P normalized with respect to the rated power $P_r = 5$ MW. The output of the LP-PIESC is the estimate of the optimal tip-speed ratio ($\hat{\lambda}$). A rate limit of 0.1/s is applied to the estimated optimal tip-speed ratio to produce the actual TSR set-point (λ_{sp}) for the ROSCO controller (λ_{opt} in Figure 1).

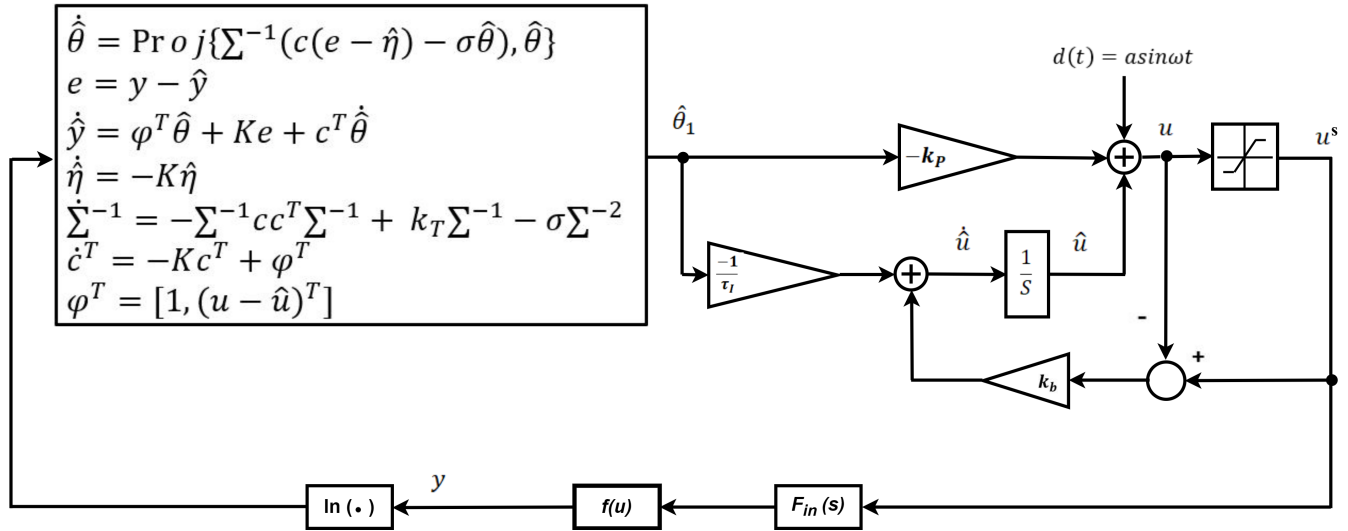


Figure 5. LP-PIESC: PIESC with log power feedback and integrator anti-windup.

Table 1. Main parameters of NREL 5MW turbine.

Description	Value
Rated Power	5 MW
Rotor radius (R)	63 m
Gear Ratio (N)	97
Cut-in, Rated, Cut-out wind speed	3 m/s, 11.4 m/s, 25 m/s
Cut-in, Rated rotor speed	6.9 rpm, 12.1 rpm

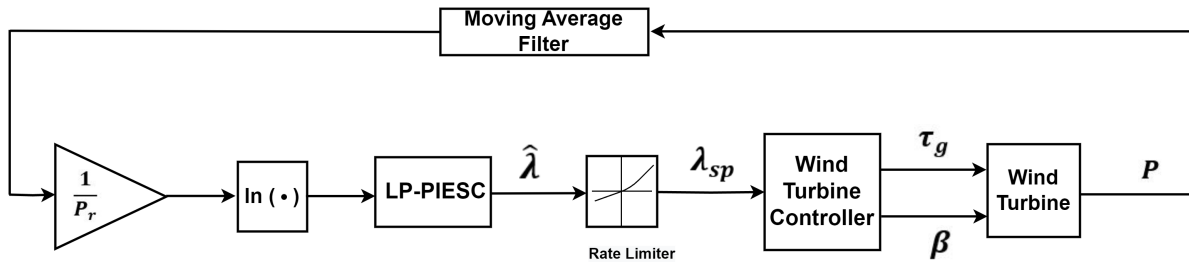


Figure 6. LP-PIESC implementation with ROSCO wind turbine controller.

The LP-PIESC parameters (Figure 5) are designed using a clean blade (no contamination or erosion) and then
 155 fixed at these design values for implementation with the degraded blade cases. First the most relevant dynamics
 is identified using step responses to select dither frequency and amplitude. Then, the remaining parameters of the



LP-PIESC are calibrated to achieve convergence to the optimum TSR for the clean blade at 8 m/s wind speed and with 10% turbulence intensity. Further details of the parameter design procedure can be found on appendix A.

3.2 Results

160 3.2.1 Simulation conditions

The LP-PIESC controller with the parameters shown in Table 2 is evaluated with OpenFAST simulations for hub-height mean wind speeds of 7 m/s, 8 m/s, and 9 m/s, vertical shear exponent $\alpha = 0.2$ and under turbulence intensities of 10% and 15%, respectively.

Table 2. Parameters of NREL 5MW LP-PIESC shown in Figure 5.

Parameter	Tip-Speed Ratio LP-PIESC
Dither Frequency (ω)	0.16 rad/s
Dither Amplitude (a)	0.1 (non-dim.)
k_T	25 rad/s
K	20 rad/s
σ	10^{-6} (s/rad) ²
k_p	3×10^{-6} s/rad
τ_I	2.1 (non-dim.)
k_b	1 rad/s

The wind profiles for the simulations were obtained using NREL TurbSim (Jonkman, 2009). TurbSim follows IEC
165 61400-1 (IEC, 2005) to generate the wind profiles. We specified five parameters in the TurbSim input file to generate the wind input files for our simulations: (1) Turbulence model is chosen as Kaimal (IECKAI), (2) IEC turbulence type is set as Normal Turbulence Model (NTM), (3) Hub-height is 90 m for NREL 5MW reference turbine, (4) Mean wind speed, and (5) Turbulence intensity in percentage. All other parameters were left to their default values in TurbSim. The mathematical expression for the Kaimal spectrum can be found in IEC (2019).

170 Figure 7 illustrates the time series of the hub-height wind speeds with means of 7 m/s, 8 m/s, and 9 m/s and 10% turbulence intensity (TI). We use these wind profiles to evaluate the performance of the LP-PIESC for both the contaminated blade case and the eroded blade case (from section 2.2). We also simulate cases with 15% TI and same mean values. In all simulations, we set the tip-speed ratio input to the ROSCO at the clean blade optimum; i.e., $\lambda_{opt} = 7.6$, for the first 500 s of the simulation and then turn on the LP-PIESC to evaluate the convergence of
175 the TSR to the new optimal values for contaminated and eroded blades, respectively.

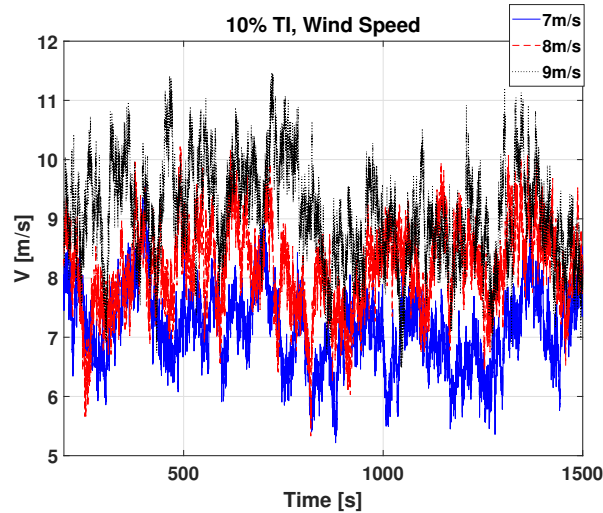


Figure 7. Wind speed time series at hub height: mean wind speeds 7m/s, 8m/s, 9m/s and 10% turbulence intensity.

3.2.2 Simulation Results

Results for the contaminated blade with the wind profile in Figure 7 are shown in Figure 8. The top plot shows the tip-speed ratio set-point (λ_{sp}) given to the ROSCO (see Figure 6), the middle plot shows the actual tip-speed ratio (λ) output and the estimated power coefficient (C_P) is shown in the bottom plot; these latter two parameters are from OpenFAST. Both the tip-speed ratio (λ) and the power coefficient (C_P) time series are shown after applying a 100 s moving average filter to the OpenFAST outputs to smooth these signals. Recall from Figure 4 that the optimal value of the tip-speed ratio and the maximum value of C_P for this case are 8.2 and 0.431, respectively.

The LP-PIESC converges to the new optimal tip-speed ratio almost instantaneously for all the cases. The actual tip-speed ratio (λ) and the estimated power coefficient (C_P) converge in less than 100 s. With 9 m/s mean wind speed there are some drops in the estimated power-coefficient (C_P) around 500 s, 800 s and 1400 s. From Figure 7, we can see that during those instances the wind speed moves into above-rated operation of the NREL 5-MW turbine (Jonkman et al., 2009). This can also be seen from Figure 9 where the blade pitch (bottom right plot) is activated at those times to regulate the generator speed close to its rated value 1173.7 rpm. The increase to above-rated wind speed, and approximate regulation of generator speed provided by ROSCO, explain the dips observed in power coefficient and tip-speed ratio in Figure 8.

We also evaluate the performance of the LP-PIESC with an increased turbulence intensity of 15%. The simulation results are shown in Figure 10. It is observed that increasing the turbulence intensity does not affect the transient or steady-state performance of the LP-PIESC. The LP-PIESC continues to converge quickly, and the drop in C_P for 9 m/s wind speed is due to the turbine entering the above-rated wind speed region.

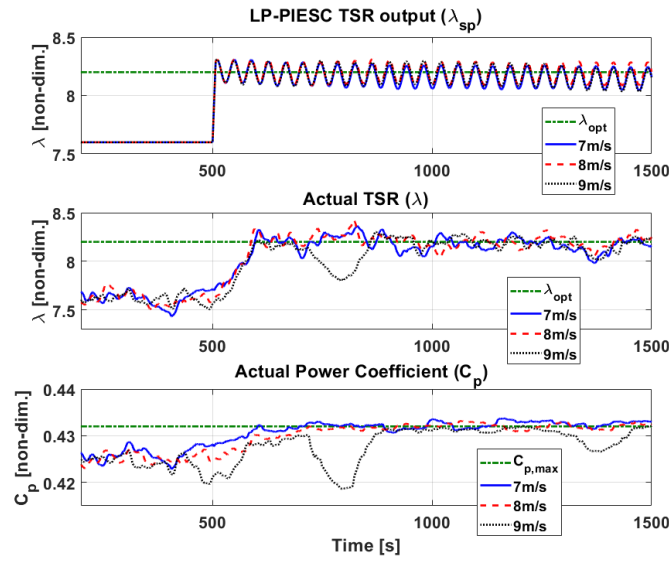


Figure 8. Contaminated blade - Performance of the LP-PIESC with the parameters in Table 2 and hub-height wind speed from Figure 7. The LP-PIESC is turned on at 500 s. Rate-limited LP-PIESC tip-speed ratio set-point λ_{sp} (**top**), tip speed ratio from OpenFAST output λ (**middle**), estimated power coefficient C_P (**bottom**). The dashed green horizontal lines indicate true optimal parameters λ_{opt} , and $C_{P,max}$ (Figure 4).

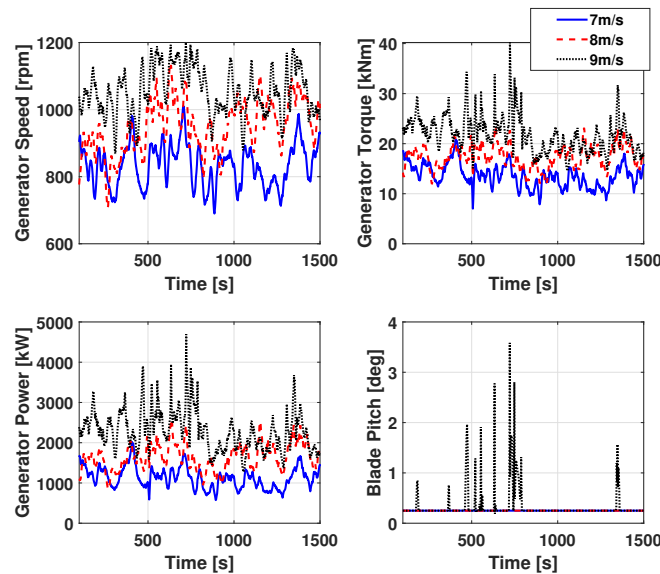


Figure 9. Contaminated blade - Response of turbine parameters with the LP-PIESC and the wind profiles in Figure 7.

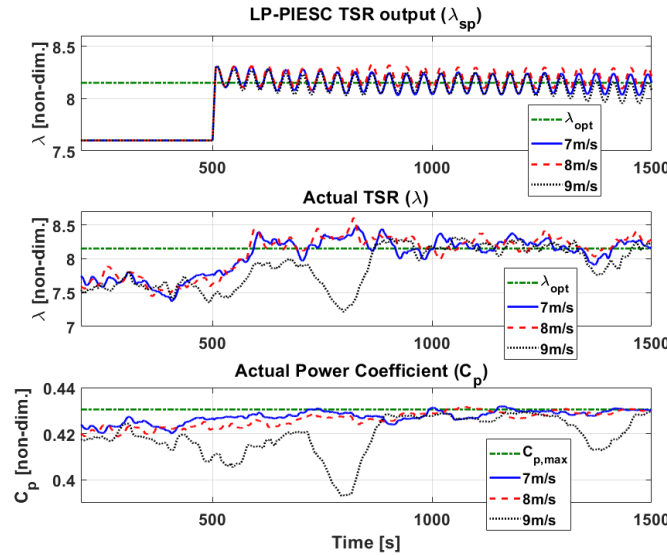


Figure 10. Contaminated blade - Performance of the LP-PIESC with the parameters shown in Table 2 and wind input with 15% TI. The LP-PIESC is turned on at 500 s. Rate-limited LP-PIESC tip-speed ratio set-point λ_{sp} (**top**), tip speed ratio from OpenFAST output λ (**middle**), estimated power coefficient C_p (**bottom**). The dashed green horizontal lines indicate true optimal parameters λ_{opt} , and $C_{p,max}$ (Figure 4).

195 Next, we evaluate the performance of the LP-PIESC for the eroded blade case using the same mean wind speeds and turbulence intensity as before. Recall from Figure 4 that the optimal value of the tip-speed ratio and the maximum value of C_p for this case are 8.4 and 0.351, respectively. Results for this case are shown in Figure 11 and 12. It can be observed that as the LP-PIESC is turned on at 500 s, it converges to the optimal tip-speed ratio almost instantaneously for all the cases. The drops in C_p for 9 m/s mean wind speed can be explained as before.

200 *The results in this section provided evidence that the LP-PIESC quickly finds the unknown optimal tip-speed ratio despite variations in mean wind speed, turbulence intensity, and the level of blade degradation.*

3.2.3 Energy Capture

The energy capture using the LP-PIESC for both the contaminated blade case and the eroded blade case (Figure 4) is evaluated and compared with the baseline controller (i.e., the controller with the tip-speed ratio constant and corresponding to clean blades). The controllers are evaluated for hub-height mean wind speeds of 7 m/s, 8 m/s, and 205 9 m/s, vertical shear exponent $\alpha=0.2$ and turbulence intensities of 10% and 15%, respectively. TurbSim (Jonkman, 2009) is used to generate the wind profiles from six different seeds for each wind speed and turbulence intensity. An average energy capture over those six wind profiles is presented here. All the calculations are done using the data from the time LP-PIESC is turned on (500 s) till the end of the simulation (1500 s).

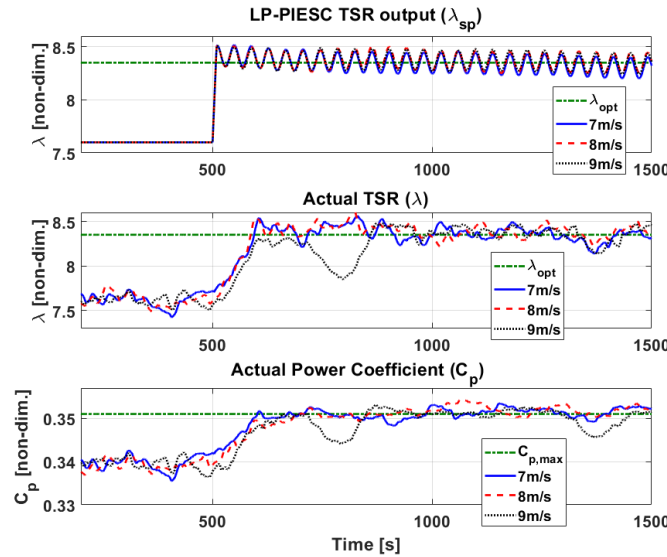


Figure 11. Eroded blade - Performance of the LP-PIESC with the parameters shown in Table 2 and hub-height wind from Figure 7. The LP-PIESC is turned on at 500 s. Rate-limited LP-PIESC tip-speed ratio set-point λ_{sp} (**top**), tip speed ratio from OpenFAST output λ (**middle**), estimated power coefficient C_p (**bottom**). The dashed green horizontal lines indicate true optimal parameters λ_{opt} , and $C_{p,max}$ (Figure 4).

210 The contaminated blade case is shown in Figure 13. The average energy capture with the LP-PIESC is compared with that of the baseline controller. Both the controllers were applied to the same blades (contaminated for this case). The baseline controller applies a constant tip-speed ratio $\lambda_{opt} = 7.6$ to ROSCO while the LP-PIESC applies the optimized tip-speed ratio time series λ_{sp} from Figures 8 and 10. The energy capture with the LP-PIESC for the eroded blade was also compared with the baseline controller using the same approach. The average energy capture
 215 comparison for the eroded blade is shown in Figure 14.

The results suggest that the LP-PIESC could find the unknown optimal tip-speed ratio for off-design conditions and improve the energy capture. The maximum improvement is observed with the mean wind speed of 7 m/s, 10% TI wind for both the contaminated (1.5%) and the eroded blade (3.4%) cases. It is interesting to note that these improvements in energy capture are very close to the reported improvements in the power coefficient in Section 2.2
 220 as explained in the caption of Figure 4. The percentage energy increase for the mean wind speed of 9 m/s was the lowest. In this case, turbulence takes the wind speed and generator speed in the above-rated region where the turbine blade-pitch controller gets activated to constrain the generated speed to the rated value.

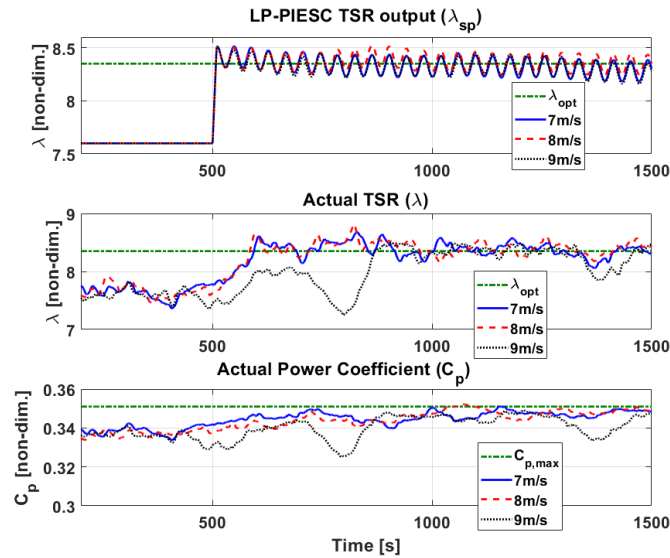


Figure 12. Eroded blade - Performance of the LP-PIESC with the parameters shown in Table 2 and wind input with 15% TI. The LP-PIESC is turned on at 500 s. Rate-limited LP-PIESC tip-speed ratio set-point λ_{sp} (**top**), tip speed ratio from OpenFAST output λ (**middle**), estimated power coefficient C_P (**bottom**). The dashed green horizontal lines indicate true optimal parameters λ_{opt} , and $C_{P,max}$ (Figure 4).

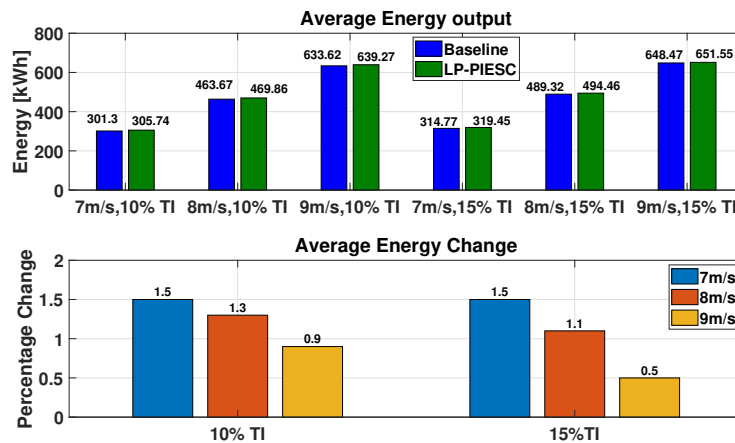


Figure 13. Contaminated blade - Energy capture comparison: Baseline vs. LP-PIESC. Average energy output with clean-blade optimal tip-speed ratio and LP-PIESC (**top**), percentage change in energy capture (**bottom**).

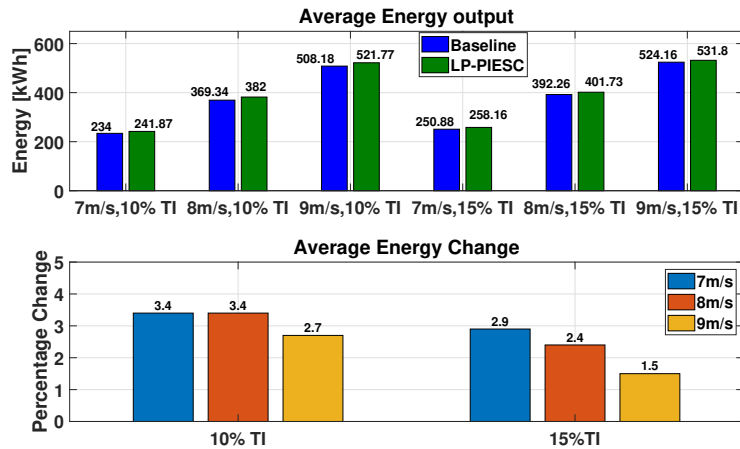


Figure 14. Eroded blade - Energy capture comparison: Baseline vs. LP-PIESC. Average energy output with clean-blade optimal tip-speed ratio and LP-PIESC (**top**), percentage change in energy capture (**bottom**).

4 Conclusions

A log-power feedback PIESC (LP-PIESC) algorithm is presented to estimate the optimal tip speed ratio (TSR) below rated wind speeds despite changes in the rotor aerodynamics. Knowledge of the optimal TSR is necessary when the wind turbine controller uses this information to adjust the rotor speed for optimal power extraction such as the ROSCO reference controller introduced in Abbas et al. (2022).

Simulation results show that LP-PIESC can identify the optimal tip ratio for blades with contaminated or eroded airfoils despite variations in mean wind speed or turbulence intensity. The simulations show that re-tuning the TSR to optimal values can lead to increases in energy capture ranging from 0.5% to 1.5 % for contaminated blades and from 1.5% to 3.4% for eroded blades. The highest energy increases occur at lower wind speeds, which is a favorable situation. Energy increases with eroded blades are higher than with contaminated blades for all cases considered. These positive results need to be balanced with the fact that for both contaminated and eroded blades optimal TSRs increase, which requires higher rotor speeds. The implications of this fact on the progression of blade degradation would need to be better understood. However, the method proposed can be used to increase energy capture until blades need to be cleaned or repaired.

The LP-PIESC technique provides rapid and consistent convergence across different below-rated wind speed conditions. Calibration of algorithm parameters at one wind condition works at other wind conditions. However, the design of the PIESC algorithm requires tuning more parameters than the conventional ESC. Therefore, additional work is needed to establish practical guidelines for parameter design. It is also important to note that if the turbine controller requires the $C_p - \lambda$ curve for wind speed estimation or another control function, then estimating the



optimal TSR set-point under blade degradation may not suffice to realize power gains; additional parameters would need to be estimated in this case to optimize power for aerodynamically degraded rotors.

Code availability. Not Applicable

245 *Data availability.* The data presented in this work can be made available upon request.

Appendix A: Parameter design for the NREL 5-MW reference turbine

The LP-PIESC parameters are designed using a clean blade (no contamination or erosion) and then fixed at these design values for the degraded blade cases, which would be a reasonable way of deploying the algorithm in the field. First the most relevant dynamics is identified using step responses to select dither frequency and amplitude. Then,
250 the remaining parameters of the LP-PIESC are calibrated to achieve fast convergence to the optimum TSR for the clean blade at 8 m/s wind speed and with 10% turbulence intensity.

Following the ESC design guidelines in Ariyur and Krstic (2003); Rotea (2000), the dither frequency is chosen within the bandwidth of the plant dynamics. The rotor inertia and the actuator dynamics yield the input dynamics. The input dynamics is merged with the plant and estimated using open-loop step responses under constant wind
255 input to simplify the algorithm design. The response of the rotor speed (ω_r) under staircase step changes in the tip-speed ratio indicates a second-order dynamics (a first-order wind turbine dynamics and the dynamics of the generator torque PI controller), as shown in Figure A1. The top plot in Figure A1 shows the staircase tip-speed ratio command to the ROSCO and the OpenFAST tip-speed ratio output, while the rotor speed is shown in the bottom plot. The test was performed for the hub-height mean wind speed of 8 m/s with no turbulence. Based on the
260 step response of the rotor speed, natural frequency (ω_n) and damping ratio (ζ) were calculated for each step change case. ω_n ranged between 0.36 rad/s to 0.5 rad/s while ζ ranged between 0.56 to 0.77. Then we calculated the time constant (i.e., $\tau = \frac{1}{\zeta\omega_n}$) for each case and the slowest combination (i.e., largest time constant) was adopted for the LP-PIESC design, i.e., $\omega_n = 0.36$ rad/s and $\zeta = 0.76$. The corresponding bandwidth of the tip-speed ratio LP-PIESC is 0.33 rad/s. Since dither frequency should be selected within the estimated bandwidth, it was selected as 0.16 rad/s.
265 The Bode plot for the estimated plant dynamic is shown in Figure A2. The dither amplitude was selected using trial and error. The parameters of the LP-PIESC scheme are listed in Table A1. The minimum and maximum saturation limits for the tip-speed ratio set-point were set at 4 and 10 (Figure 5). The remaining LP-PIESC parameters were calibrated with the clean blade to achieve fast convergence for the 8 m/s wind speed with 10% turbulence intensity (TI), and then these parameters were used in all simulations.

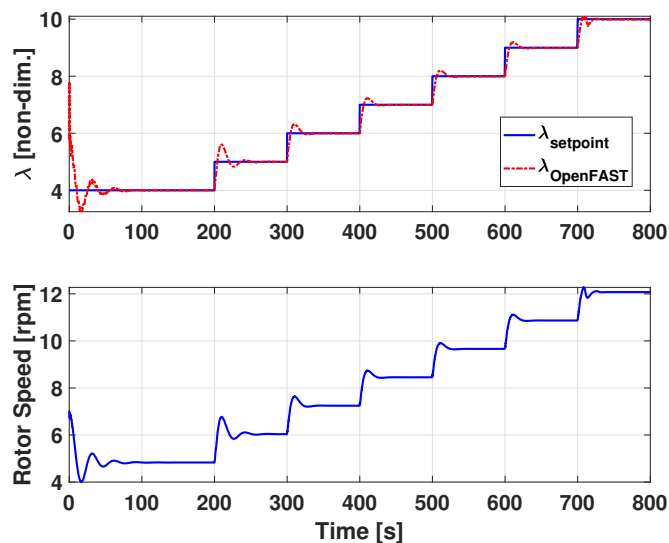


Figure A1. The top plot shows the staircase tip-speed ratio command to the ROSCO and the OpenFAST tip-speed ratio output while the bottom plot shows the rotor speed response.

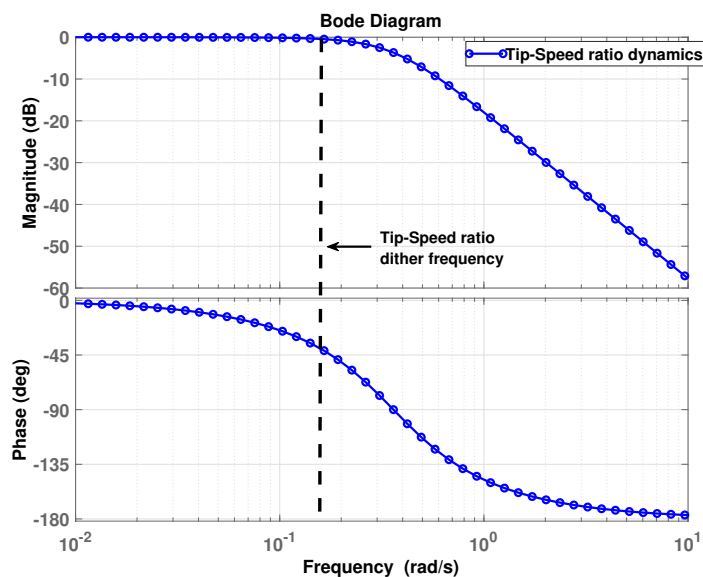


Figure A2. Bode plot of input dynamics, and the dither frequency.

270 *Author contributions.* DK: Data curation, Formal analysis, Investigation, Software, Visualization, Writing - original draft preparation. MR: Conceptualization, Funding acquisition, Methodology, Resources, Supervision, Visualization, Writing - review & editing.



Table A1. LP-PIESC Parameters of NREL 5MW below-rated tip-speed ratio controller. See Figure (5).

Parameter	Tip-Speed Ratio LP-PIESC
Dither Frequency (ω)	0.16 rad/s
Dither Amplitude (a)	0.1 (non-dim.)
k_T	25 rad/s
K	20 rad/s
σ	10^{-6} (s/rad) ²
k_p	0.000003 s/rad
τ_I	2.1 (non-dim.)
k_b	1 rad/s

Competing interests. No competing interests are present.

Acknowledgements. This work was supported in part by the Center for Wind Energy at the University of Texas at Dallas.



275 References

- Abbas, N. J., Zalkind, D. S., Pao, L., and Wright, A.: A reference open-source controller for fixed and floating offshore wind turbines, *Wind Energy Science*, 7, 53–73, <https://doi.org/10.5194/wes-7-53-2022>, 2022.
- Ariyur, K. B. and Krstic, M.: Real-time optimization by extremum-seeking control, John Wiley & Sons, 2003.
- Burton, T., Jenkins, N., Sharpe, D., and Bossanyi, E.: *Wind energy handbook*, John Wiley & Sons, 2011.
- 280 Ciri, U., Leonardi, S., and Rotea, M. A.: Evaluation of log-of-power extremum seeking control for wind turbines using large eddy simulations, *Wind Energy*, 22, 992–1002, 2019.
- Creaby, J., Li, Y., and Seem, J. E.: Maximizing Wind Turbine Energy Capture Using Multivariable Extremum Seeking Control, *Wind Engineering*, 33, 361–387, 2009.
- Ehrmann, R. S., White, E. B., Maniaci, D. C., Chow, R., Langel, C. M., and Van Dam, C. P.: Realistic leading-edge roughness effects on airfoil performance, in: 31st AIAA Applied Aerodynamics Conference, p. 2800, 2013.
- 285 Ehrmann, R. S., Wilcox, B., White, E. B., and Maniaci, D. C.: Effect of Surface Roughness on Wind Turbine Performance., Tech. rep., Sandia National Lab.(SNL-NM), Albuquerque, NM (United States), 2017.
- Guay, M. and Dochain, D.: A proportional-integral extremum-seeking controller design technique, *Automatica*, 77, 61 – 67, 2017.
- 290 Han, W., Kim, J., and Kim, B.: Effects of contamination and erosion at the leading edge of blade tip airfoils on the annual energy production of wind turbines, *Renewable Energy*, 115, 817–823, <https://doi.org/https://doi.org/10.1016/j.renene.2017.09.002>, 2018.
- IEC: Wind energy generation systems—part 1: design requirements, 2005.
- IEC: Wind energy generation systems-Part 1: Design requirements, International Electrotechnical Commission, Geneva, 295 Switzerland, 2019.
- Jonkman, B. J.: TurbSim user’s guide: Version 1.50, Tech. rep., National Renewable Energy Lab.(NREL), Golden, CO (United States), <https://www.nrel.gov/docs/fy09osti/46198.pdf>, 2009.
- Jonkman, J.: The New Modularization Framework for the FAST Wind Turbine CAE Tool, in: 51st AIAA Aerospace Sciences Meeting including the New Horizons Forum and Aerospace Exposition, AIAA 2013-0202, pp. 1–26, <https://arc.aiaa.org/doi/abs/10.2514/6.2013-202>, 2013.
- 300 Jonkman, J., Butterfield, S., Musial, W., and Scott, G.: Definition of a 5-MW reference wind turbine for offshore system development, Tech. rep., National Renewable Energy Lab.(NREL), Golden, CO (United States), <https://www.nrel.gov/docs/fy09osti/38060.pdf>, 2009.
- Kumar, D. and Rotea, M. A.: Wind Turbine Power Maximization Using Log-Power Proportional-Integral Extremum Seeking, *Energies*, 15, <https://doi.org/10.3390/en15031004>, 2022.
- 305 Manwell, J. F., McGowan, J. G., and Rogers, A. L.: *Wind energy explained: theory, design and application*, John Wiley & Sons, 2010.
- NREL: OpenFAST, Version 2.3.0, GitHub [code], <https://github.com/OpenFAST/openfast>, 2020, accessed: October 10, 2023).
- Pao, L. Y. and Johnson, K. E.: Control of Wind Turbines, *IEEE Control Systems*, 31, 44–62, <https://ieeexplore.ieee.org/document/5730721>, 2011.
- 310



- Rotea, M. A.: Analysis of multivariable extremum seeking algorithms, in: Proceedings of the 2000 American Control Conference. ACC (IEEE Cat. No.00CH36334), vol. 1, pp. 433–437, 2000.
- Rotea, M. A.: Logarithmic Power Feedback for Extremum Seeking Control of Wind Turbines, IFAC-PapersOnLine, 50, 4504 – 4509, 20th IFAC World Congress, 2017.
- 315 Wilcox, B. and White, E.: Computational analysis of insect impingement patterns on wind turbine blades, Wind Energy, 19, 483–495, <https://doi.org/https://doi.org/10.1002/we.1846>, 2016.
- Wilcox, B. J., White, E. B., and Maniaci, D. C.: Roughness sensitivity comparisons of wind turbine blade sections, Albuquerque, NM, 2017.
- Zanon, A., De Gennaro, M., and Kühnelt, H.: Wind energy harnessing of the NREL 5 MW reference
320 wind turbine in icing conditions under different operational strategies, Renewable Energy, 115, 760–772, <https://doi.org/https://doi.org/10.1016/j.renene.2017.08.076>, 2018.